

Optical Response of LEKID Arrays

Shibo Shu^{1*}, Martino Calvo², Johannes Goupy², Andrea Catalano^{2,3}, Aurelien Bideaud², Alessandro Monfardini², Samuel Leclercq¹ and Eduard F.C. Driessen¹

¹*Institut de Radioastronomie Millimétrique, 300 rue de la Piscine, Domaine Universitaire, 38406 Saint Martin d'Hères, France*

²*Institut Néel, CNRS and Université Grenoble Alpes, 25 av. des Martyrs, 38042 Grenoble, France*

³*Laboratoire de Physique Subatomique et de Cosmologie, Université Grenoble Alpes, CNRS, 53 av. des Martyrs, Grenoble, France*

*Contact: shu@iram.fr

Abstract—We present an analysis of the optical response of lumped-element kinetic-inductance arrays, using the NIKA2 1mm array as an example. This array design has a dual-polarization sensitive Hilbert inductor for directly absorbing incident photons. We calculated the optical response from a transmission line model and compared it with simulation using HFSS. From the simulation, we noticed that a non-negligible part of energy is reflected as higher modes. We show the difficulty of achieving high absorption rate using aluminum. This analysis could be extended to other kinetic inductance detector array designs in millimeter, sub-millimeter and terahertz frequency bands.

I. INTRODUCTION

To detect weak astronomical signals, superconducting devices such as kinetic inductance detectors (KIDs) [1] and transition edge detectors (TESs) [2], are widely developed for many astrophysics applications in millimeter, sub-millimeter, and far-infrared wavelength bands [3]-[7]. For total-power detection, usually a large number of pixels is required to increase the observation efficiency [8]. For example, the SCUBA2 [9] has 10^4 pixels and the OST satellite [10] requires 10^5 pixels for its far-infrared imager. In the astronomical detection field, KIDs have attracted great interest and have been developed rapidly in the last decade. Compared with TESs, the main advantages of KIDs are their simple structure and the intrinsic frequency domain multiplexing property. KIDs are based on superconducting microresonators [11], coupled capacitively or inductively to a feedline for frequency multiplexing. When the energy of incident photon is larger than the superconducting gap ($h\nu > 2\Delta$), the Cooper pairs are broken and quasi-particles are generated. This increases the kinetic inductance and the loss in the superconductor. The increased kinetic inductance shifts the resonance frequency and the increased loss decreases the resonance dip. Both can be read out from the resonance curve. Using a single feedline, hundreds or even thousands of KIDs can be read out simultaneously.

For lumped-element KIDs (LEKIDs) [12], Roesch et al. [13] have investigated the optical response of a LEKIDs array in the 2 mm atmospheric band. In their model, the array

consists of a set of periodic pixels only, and the readout line is not considered. The absorption rate is calculated from the return loss measured using a vector network analyzer. In their analysis the simulation and measurement matched well, however, the simulation is done assuming a waveguide boundary and the higher modes are not considered.

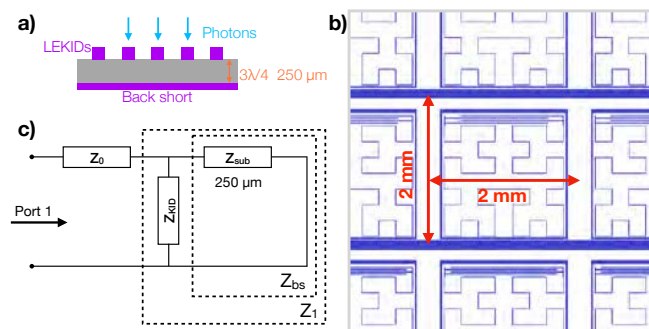


Fig. 1. a) Cut view of the LEKIDs array in the photon incident direction. b) Schematic drawing of the NIKA2 1mm array. The pitch size is 2 mm. c) Transmission line model of the optical coupling in (a). The LEKID, mainly the inductor, is represented by a sheet impedance Z_{KID} .

II. ARRAY LAYOUT

The NIKA2 1mm LEKIDs array [5] (Fig. 1) is simulated in this article. This array consists of 1140 pixels read out by 8 microstrip feedlines. The size of the array is a circle with radius of 40 mm corresponding to a 6.5° field-of-view on the IRAM 30-m telescope. The pixel pitch size and the inductor size are $2 \times 2 \text{ mm}^2$ and $1.6 \times 1.5 \text{ mm}^2$, respectively. The pixels are placed repeatedly with the same inductor design but different capacitor finger lengths for different designed resonance frequencies. The back of the wafer is covered with 200 nm thick aluminum, and acts at the same time as the ground plane for the MS readout feedline and as the backshort to optimize the optical coupling.

This array uses the bare LEKID design, which has no antenna structure on the focal plane. The incident light illuminates the array directly. The detection band of the

LEKIDs is determined by the backshort distance, which is the thickness of the silicon substrate. The band central frequency (wavelength) is designed to be 260 GHz (1.15 mm), the central frequency of the 260 GHz atmospheric window. The backshort is designed to be $3\lambda_{\text{Si}}/4=250 \mu\text{m}$, where the wavelength in silicon $\lambda_{\text{Si}} = \lambda/\sqrt{\epsilon_r}=333 \mu\text{m}$, the wavelength in free space $\lambda=1.15 \text{ mm}$ and the relative permittivity of silicon $\epsilon_r=11.9$.

The inductor is designed with a 3rd-order Hilbert curve [14] for dual-polarization sensitivity. The inductor width and the interval distance are designed as $s=4 \mu\text{m}$ and $w=240 \mu\text{m}$, respectively. Since the wavelength is much larger than the structure, the inductor can be simplified as a sheet impedance Z_{KID} . The optical coupling can be modeled using the transmission line model [15], shown in Fig. 1 (c). The impedance of the backshort can be expressed as

$$Z_{\text{bs}} = jZ_{\text{sub}} \tan(\beta l),$$

where $\beta = 2\pi/\lambda_{\text{Si}}$ and l is the backshort distance (250 μm). The effective impedance of the KIDs together with the backshort is

$$Z_1 = \frac{1}{\frac{1}{Z_{\text{KID}}} + \frac{1}{Z_{\text{bs}}}}.$$

Assuming the reactance is zero, the impedance of KID is

$$Z_{\text{KID}} = R_{\text{sq}}/(s/w).$$

Then the absorption rate is calculated as

$$\text{absorption rate} = 1 - |S_{11}|^2 = 1 - \left| \frac{Z_0 - Z_1}{Z_0 + Z_1} \right|^2,$$

where the vacuum impedance $Z_0 = 377 \Omega$. Given the sheet resistance $R_{\text{sq}} = 1.6 \Omega/\text{sq}$ of the used 20 nm aluminum film, $Z_{\text{KID}} = 96 \Omega$ and the maximum absorption is 64.7% at the band center. This is only a simple estimation for the absorption rate. Actually, away from the band center, the absorption rate largely depends on the reactance of Z_{KID} , which is usually not zero and cannot be evaluated analytically. Therefore, we use the electromagnetic simulation as a useful tool for focal plane array design.

III. SIMULATION

The simulations are done using HFSS [16]. A Floquet port is assigned to Port 1 for exciting plane waves (Fig. 2). Considering the simulating frequency from 150 to 350 GHz, 18 modes are included in the analysis. Two TEM modes, TE00 and TM00 with y and x -axis polarizations, respectively, are simulated as the incident signal.

The surfaces of all components of pixel are assigned with an impedance boundary in the simulation. The simulated S-parameters are shown in Fig. 2 (b) and (c) for incident polarization 1 and 2, respectively. For the clarity of the discussion, only the modes with maximum values larger than -20 dB are considered and plotted.

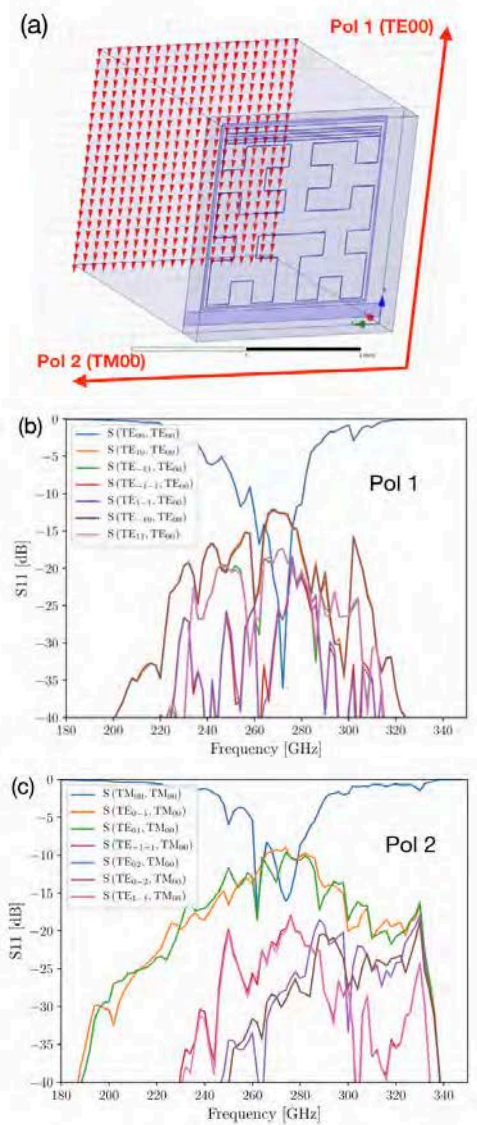


Fig. 2. a) The simulation model of a single pixel in HFSS. Two polarizations (TE00 and TM00) are stimulated as the incident signal. The arrows show the direction of the electric field in the two dominant modes. b) S-parameter results for a TE00 excitation (Pol 1). Only the modes with a maximum return loss higher than -20 dB are plotted for clarity (same for (c)). The TE10 and TE-10 modes have more reflect energy than other higher modes. c) S-parameter results for a TM00 excitation (Pol 2). TE0-1 and TE01 modes reflect more energy than other higher modes.

From the S11 of the dominant mode, the band center is -36 dB at 272 GHz and -17.5 dB at 274 GHz for Pol 1 and Pol 2, respectively. Compared with the design central frequency 260 GHz, there is a 12 GHz difference. The total absorption rate has a maximum at 262 GHz for both polarizations, which is consistent with the design. This analysis shows that actually a non-negligible part of the energy is reflected into higher modes, which are not considered in earlier studies [14].

The two dominant reflected higher modes are TE10 and TE-10 for Pol 1 and TE0-1 and TE01 for Pol 2. The maximum reflection of all higher modes together is 15.1% and 27.2% for Pol 1 and Pol 2, respectively. The average reflection in band

from 230 to 290 GHz of all higher modes is 6.3% and 13.0% for Pol 1 and Pol 2, respectively. A large portion of the reflected higher modes is due to the reflected energy by impedance mismatch, 35.3% at peak calculated using the transmission line model. We also find that the electric field distributions of these higher modes for both polarizations are consistent with the geometry of the Hilbert curve. This suggests that part of the higher modes is caused by the non-uniformity of the inductor geometry. Compared to the wavelength 1.15 mm, the segment length of 240 μm is quite large ($\lambda/5$). Ideally the typical geometry should be much smaller than the wavelength to be treated as a uniform sheet ($\ll \lambda/10$) [17]. However, decreasing the segment length will also decrease the inductor width, resulting in a decrease of array yield and uniformity. For example, if we increase the third-order Hilbert inductor to a fourth order, the inductor width will be around 1 μm , and the total length of the inductor will be 27 cm. To fabricate such long and narrow line is a challenge for the yield of fabrication.

CONCLUSIONS

We have presented a transmission line model for our test LEKID array. Simulation results show that there is a non-negligible part of energy reflected to higher modes. Using low resistivity material, like aluminum, there may be a fabrication problem for achieving the maximum absorption rate. We are currently working on the extraction of the energy absorbed by the individual components, like the inductor, and optical response measurements. Further results are under investigation.

ACKNOWLEDGMENT

We thank Alvaro Gonzalez, Tom Nitta and Wenlei Shan for useful discussion and Yutaro Sekimoto for encouragement. The HFSS simulations were performed at National Astronomical Observatory of Japan.

REFERENCES

- [1] P. K. Day, H. G. LeDuc, B. A. Mazin, A. Vayonakis, and J. Zmuidzinas, "A broadband superconducting detector suitable for use in large arrays," *Nature*, vol. 425, no. 6960, p. 817, 2003.
- [2] K. D. Irwin and G. C. Hilton, "Transition-edge sensors," in *Cryogenic particle detection*. Springer, 2005, pp. 63–150.
- [3] A. Monfardini, L. J. Swenson, A. Bideaud, F. X. Desert, S. J. C. Yates, A. Benoit, A. M. Baryshev, J. J. A. Baselmans, S. Doyle, B. Klein, M. Roesch, C. Tucker, P. Ade, M. Calvo, P. Camus, C. Giordano, R. Guesten, C. Hoffmann, S. Leclercq, P. Mauskopf, and K. F. Schuster, "NIKA: A millimeter-wave kinetic inductance camera," *Astronomy and Astrophysics*, vol. 521, p. A29, Oct. 2010.
- [4] J. Sayers, C. Bockstiegel, S. Brugger, N. G. Czakon, P. K. Day, T. P. Downes, R. P. Duan, J. Gao, A. K. Gill, J. Glenn et al., "The status of music: the multiwavelength sub-millimeter inductance camera," in *Millimeter, Submillimeter, and Far-Infrared Detectors and Instrumentation for Astronomy VII*, vol. 9153. International Society for Optics and Photonics, 2014, p. 915304.
- [5] R. Adam, A. Adane, P. Ade, P. Andre, A. Andrianasolo, H. Aussel, A. Beelen, A. Benoit, A. Bideaud, N. Billot et al., "The nika2 large-field-of-view millimetre continuum camera for the 30-m iram telescope," *Astronomy & Astrophysics*, vol. 609, p. A115, 2018.
- [6] L. Ferrari, O. Yurduseven, N. Llombart, S.J.C. Yates, A.M. Baryshev, J. Bueno, and J. J. A. Baselmans, "Performance verification of a double-slot antenna with an elliptical lens for large format KID arrays," *SPIE Astronomical Telescopes + Instrumentation*, vol. 9914, pp. 99 142G–99 142G–6, Jul. 2016.
- [7] J. Hubmayr, J. Beall, D. Becker, H.-M. Cho, M. Devlin, B. Dober, C. Groppi, G. C. Hilton, K. D. Irwin, D. Li et al., "Photon-noise limited sensitivity in titanium nitride kinetic inductance detectors," *Applied Physics Letters*, vol. 106, no. 7, p. 073505, 2015.
- [8] D. Farrah, K. Ennico Smith, D. Ardila, C. M. Bradford, M. Dipirro, C. Ferkinhoff, J. Glenn, P. Goldsmith, D. Leisawitz, T. Nikola, N. Rangwala, S. A. Rinehart, J. Staguhn, M. Zemcov, J. Zmuidzinas, J. Bartlett, S. Carey, W. J. Fischer, J. Kamenetzky, J. Kartaltepe, M. Lacy, D. C. Lis, E. Lopez-Rodriguez, M. MacGregor, S. H. Moseley, E. J. Murphy, A. Rhodes, M. Richter, D. Rigopoulou, D. Sanders, R. Sankrit, G. Savini, J.-D. Smith, and S. Stierwalt, "Review: Far-Infrared Instrumentation and Technology Development for the Next Decade," *ArXiv e-prints*, Sep. 2017.
- [9] W. Holland, D. Bintley, E. Chapin, A. Chrysostomou, G. Davis, J. Dempsey, W. Duncan, M. Fich, P. Friberg, M. Halpern et al., "Scuba-2: the 10000-pixel bolometer camera on the james clerk maxwell telescope," *Monthly Notices of the Royal Astronomical Society*, vol. 430, no. 4, pp. 2513–2533, 2013.
- [10] J. Fortney, T. Kataria, K. Stevenson, R. Zellem, E. Nielsen, P. Cuartas-Restrepo, E. Gaidos, E. Bergin, M. Meixner, S. Kane et al., "The origins space telescope: Towards an understanding of temperate planetary atmospheres," *arXiv preprint arXiv:1803.07730*, 2018.
- [11] J. Zmuidzinas, "Superconducting Microresonators: Physics and Applications," *Annual Review of Condensed Matter Physics*, vol. 3, no. 1, pp. 169–214, 2012.
- [12] S. Doyle, P. Mauskopf, J. Naylor, A. Porch, and C. Duncombe, "Lumped Element Kinetic Inductance Detectors," *Journal of Low Temperature Physics*, vol. 151, no. 1, pp. 530–536, Apr. 2008.
- [13] M. J. Rosch, F. Mattiocco, T. A. Scherer, M. Siegel, and K.-F. Schuster, "Modeling and Measuring the Optical Coupling of Lumped Element Kinetic Inductance Detectors at 120–180 GHz," *IEEE Transactions on Antennas and Propagation*, vol. 61, no. 4, pp. 1939–1946, 2013.
- [14] M. Roesch, A. Benoit, A. Bideaud, N. Boudou, M. Calvo, A. Cruciani, S. Doyle, H. Leduc, A. Monfardini, L. Swenson et al., "Development of lumped element kinetic inductance detectors for nika," *arXiv preprint arXiv:1212.4585*, 2012.
- [15] M. Roesch, Development of lumped element kinetic inductance detectors for mm-wave astronomy at the IRAM 30 m telescope. KIT Scientific Publishing, 2014, vol. 12.
- [16] ANSYS HFSS Software HP: <https://www.ansys.com>
- [17] S. Doyle, "Lumped element kinetic inductance detectors," Ph.D. dissertation, Cardiff University, 2008.